ELSEVIER

Brain Research 885 (2000) 251–261

BRAIN RESEARCH

www.elsevier.com/locate/bres

Research report

Structural alterations of tight junctions are associated with loss of polarity in stroke-prone spontaneously hypertensive rat blood–brain barrier endothelial cells

Andrea Lippoldt[a,*,1], Uwe Kniesel[b,c,1], Stefan Liebner[b], Hubert Kalbacher[d], Torsten Kirsch[a], Hartwig Wolburg[b], Hermann Haller[e]

[a]*Max-Delbrück-Center for Molecular Medicine, Robert-Rössle-Strasse 10, 13092 Berlin, Germany*
[b]*Institute of Pathology, University of Tübingen, Tübingen, Germany*
[c]*Institute of Zoology, University of Stuttgart–Hohenheim, Stuttgart, Germany*
[d]*Medical and Natural Sciences Research Center, Tübingen, Germany*
[e]*Department of Nephrology, Medical School, Hannover, Germany*

Accepted 12 September 2000

Abstract

The mechanisms leading to stroke in stroke-prone spontaneously hypertensive rats (SHRSP) are not well understood. We tested the hypothesis that the endothelial tight junctions of the blood–brain barrier are altered in SHRSP prior to stroke. We investigated tight junctions in 13-week-old SHRSP, spontaneously hypertensive stroke-resistant rats (SHR) and age-matched Wistar–Kyoto rats (WKY) by electron microscopy and immunocytochemistry. Ultrathin sections showed no difference in junction structure of cerebral capillaries from SHRSP, SHR and WKY, respectively. However, using freeze-fracturing, we observed that the blood–brain barrier specific distribution of tight junction particles between P- and E-face in WKY (58.7±3.6%, P-face; 41.2±5.59%, E-face) and SHR (53.2±19.3%, P-face; 55.6±13.25%, E-face) was changed to an 89.4±9.9% predominant E-face association in cerebral capillaries from SHRSP. However, the expression of the tight junction molecules ZO-1, occludin, claudin-1 and claudin-5 was not changed in capillaries of SHRSP. Permeability of brain capillaries from SHRSP was not different compared to SHR and WKY using lanthanum nitrate as a tracer. In contrast, analysis of endothelial cell polarity by distribution of the glucose-1 transporter (Glut-1) revealed that its abluminal:luminal ratio was reduced from 4:1 in SHR and WKY to 1:1 in endothelial cells of cerebral capillaries of SHRSP. In summary, we demonstrate that early changes exist in cerebral capillaries from a genetic model of hypertension-associated stroke. We suggest that a disturbed fence function of the tight junctions in SHRSP blood–brain barrier endothelial cells may lead to subtle changes in polarity. These changes may contribute to the pathogenesis of stroke.

Theme: Disorders of the nervous system

Topic: Genetic models

Keywords: Hypertension; Stroke; Blood–brain barrier

1. Introduction

Hypertension plays an important role in the pathogenesis of stroke. An increase in blood pressure predisposes to stroke and about 70% of stroke patients are hypertensive [4,5,36]. However, the molecular mechanisms linking hypertension to stroke are incompletely understood. Earlier reports [9,13,37] have indicated that blood–brain barrier permeability is increased in hypertension, suggesting that permeability may be important for the development of stroke. A utilitarian animal model of stroke is the stroke-prone spontaneously hypertensive rat (SHRSP) [48]. In SHRSP, 80% of the animals develop stroke spontaneously during aging or in a defined time when given the appropriate diet [15,30,46,47]. During the development of high

*Corresponding author. Tel.: +49-30-9406-3263; fax: +49-30-9406-2110.

E-mail address: lippoldt@mdc-berlin.de (A. Lippoldt).

[1]Both authors contributed equally to this work.

0006-8993/00/$ – see front matter
PII: S0006-8993(00)02954-1

blood pressure, changes in endothelial cell function occur in the cerebral vessels of SHRSP [29,35,38,41,49]. Prior to stroke a reduction in global cerebral blood flow and cortical protein synthesis is observed [24,30]. These observations have led to a hypothetical pathologic sequel where endothelial dysfunction and subsequent formation of edema precede the development of stroke [2,17,47]. The aim of the present study was to analyze these early changes in endothelial cell function.

Specific characteristics of the blood–brain barrier endothelial cells are the tight junctions. Using freeze-fracture electron microscopy it has been found that the tight junction particles have a special distribution within the fracture faces [20], that is about 57% of the particles within the internal membrane leaflet (P-face) and about 44% of the particles within the external leaflet (E-face) of the endothelial cell membrane [19]. This distribution is a prerequisite of the maintenance of the blood–brain barrier tightness [32,44] as well as of the functional polarization of the blood–brain barrier endothelial cells [42]. These cells exhibit a specific distribution pattern of enzymes and transporter molecules to the abluminal and luminal plasma membranes, respectively. Maturation of the blood–brain barrier during embryonal development and also soon after birth leading to tightening of the barrier is accompanied by a redistribution of enzyme activities and transporter molecules to their final target membranes and it is suggested that the polarity of the endothelial cells reflects the maintenance of the fence function of their tight junctions [42]. There have been preliminary reports that enzymatic activities are shifted to the other membrane which coincide with increased permeability under pathological circumstances [42,43].

We analyzed blood–brain barrier endothelial cell tight junctions prior to the development of stroke in SHRSP to test the hypothesis that the morphology of tight junctions is altered prior to stroke. We were also interested in the expression pattern of junction-forming proteins. We analyzed endothelial cell permeability using lanthanum nitrate and endothelial cell polarity by assessing the subcellular distribution of the glucose-1 transporter (Glut-1) [1,7]. We found that an altered E-face association of tight junction particles as well as their disturbed fence function, measured by Glut-1 distribution in SHRSP blood–brain barrier endothelial cells, may lead to subtle changes in the cerebral microvessel endothelial cells thereby contributing to the susceptibility to stroke.

2. Materials and methods

2.1. Animals

SHRSP were bred in the animal facility of the Max-Delbrück-Center. The 13-weeks-old rats had no neurological symptoms and had a mean arterial blood pressure (MAP) of 161±8 mmHg. Normotensive age matched Wistar–Kyoto rats (MAP 120±9 mmHg) and hypertensive age-matched SHR (MAP 166±8 mmHg) were used as controls. The rats were housed at 12 h light–dark cycle under constant temperature conditions and received standard rat chow (0.3% sodium chloride, SSNIFF Spezialitäten GmbH, Soest, Germany) and drinking water ad libitum. The animals were sacrificed using ether anesthesia and the tissue was removed and processed according to the methods requirements. For quantitation, nine animals each were used and tissue was taken from five different regions of the cerebral cortex. For ultrathin sectioning, tissue was taken from the same rats and the same regions. The protocol was approved by local authorities corresponding to criteria of the American Physiological Society.

2.2. Light microscopic immunocytochemistry

The rats (each strain four rats) were killed by ether anesthesia; the brains were removed and snap frozen in isopentane at −35°C. The brains were sectioned at 10 μm thickness in a cryostat (CM 3000, Leica, Bensheim, Germany) and mounted onto APES (Sigma)-coated slides. Immunocytochemistry was performed using immunofluorescence technique with appropriate Cy2-labeled secondary antibodies (Dianova). The primary antibodies listed in Table 1 were used. Prior to the incubation with the primary antibodies, the sections were fixed with either 4% buffered paraformaldehyde, 1% buffered paraformaldehyde at room temperature for 10 min, methanol at −20°C for 10 min, or ethanol/acetone at 4°C for 10 min as appropriate. Thereafter, the sections were rinsed in phosphate-buffered saline (PBS) and blocked with 5% BSA for 60 min at room temperature. The incubations with the primary antibodies were made in a humidified chamber over night at 4°C in a dilution buffer consisting of PBS with 0.04% Triton X-100 and 0.36% DMSO (PDT) and 1% BSA. After washing the slides three times for 5 min in PBS, the sections were incubated with the secondary Cy2-

Table 1
Antibodies and their source[a]

Antibody	Host	Dilution	Antigen	Source
Claudin-1	Rabbit	1:200	Tight junction, transmembrane protein	Zymed
Claudin-5	Rabbit	1:1000	Tight junction, transmembrane protein	Kalbacher H. (see [21])
Occludin	Rabbit	1:400	Tight junction, transmembrane protein	Zymed
ZO-1	Rabbit	1:400	Tight junction, intracellular protein	Zymed
Glut-1	Rabbit	1:400	Blood–brain barrier Glucose-1 transporter	Sigma

[a] The table gives a short characterization of the antibodies used for immunocytochemistry, their dilutions and source.

labeled antibody diluted in PDT with 1% BSA for 1 h at room temperature. After repeated washing in PBS, the sections were mounted with Aqua Poly/Mount (Polysciences, Inc.) and examined in a Zeiss Axioplan microscope (Zeiss Oberkochen). Controls were performed by omitting the primary antibody.

2.3. Immunoelectron microscopy

After perfusion (four SHRSP and four WKY rats) (2% paraformaldehyde), the specimens were immersion-fixed (2% paraformaldehyde; 2 h at 4°C), cryoprotected in 1.8 M sucrose, and quick-frozen in nitrogen-slush (−210°C). Freeze substitution and low temperature embedding in Lowicryl HM20 (Polysciences, Inc.) was done in the AFS-System (Leica, Bensheim, Germany). Ultrathin sectioning was performed with an Ultracut R ultramicrotome (Leica, Bensheim). The primary antibody Glut-1 was obtained from the source described in Table 1. Gold-conjugated secondary antibodies were purchased from Amersham and used at a dilution of 1:40. For quantitation of Glut-1, three regions of the cerebral cortex of five SHRSP and five WKY rats were investigated. From each cortex 16 capillaries were evaluated at a final magnification of ×38,000.

2.4. Electron microscopy

Small pieces of rat brain cerebral cortex were immersion fixed in 2% HMSS-buffered glutaraldehyde (Paesel, Frankfurt, Germany), stepwise dehydrated in ethanol and block stained with saturated uranyl acetate, embedded in Araldite (Serva, Heidelberg, Germany) and sectioned on an Ultracut FCR ultramicrotome (Leica). Semithin sections (0.6 μm) were stained with Toluidine Blue, ultrathin sections were stained with lead citrate, mounted on pioloform-coated copper grids and examined in a Zeiss (EM10; Oberkochen, Germany) or LEO (EM902; Oberkochen, Germany) electron microscope.

2.5. Freeze fracture analysis

The specimens were immersion-fixed with 2.5% buffered glutaraldehyde, cryoprotected for freeze-fracture in 30% glycerol, and quick-frozen in nitrogen-slush (−210°C). Subsequently, the specimens were fractured in a Balzer's freeze-fracture unit (BAF 400D) at 5×10^{-6} mbar and −150°C and the fracture faces were shadowed with platinum/carbon (10:1; 2 nm; 45°) for contrast and carbon (20 nm; 90°) for stabilization. After removing the cell material in 12% sodium hypochlorite, the replicas were cleaned several times in double distilled water and mounted on Formvar-coated copper grids. The preparations were investigated using a Zeiss EM10 and EM902 electron microscope.

2.6. Morphometrical analysis of the tight junction network

Quantitation was done at a final magnification of 1:120,000. Tight junction-complexity was characterized by fractal analysis and complexity index [18]. For evaluation of the fractal dimension (FD), the electron microscopic image was digitized; five grids of different scaling levels (grid-sizes) were superimposed for each scaling-factor. The number of boxes containing parts of the tight junction structure were counted (N) in repeated measurements. The grid sizes were 0.2, 0.1, 0.05, 0.025, and 0.0125 μm^2. Since the definition of the FD (box counting) is $\log N/\log(1/s)$, the values obtained for each scaling-level were inserted into a logN vs. $\log(1/s)$ graph for visualization, and the regression curve was calculated. The slope of the curve gives the estimated value for the FD. The degree of membrane association of tight junction-particles was determined as the ratio 'total length' of E- or P-face associated tight junction particles or 'strands' to 'total length' of the tight junction membrane structure, in percent. For quantification, the digitized images of the tight junctions were analyzed using the morphometric software package 'AnalySIS' (SIS, Münster, Germany). The total particle density was given as E- and P-face parts of the TJ-strands in percent of the tight junction length. A total number of 234 tight junctions from cortices of nine SHRSP, 123 tight junctions from cortices from five SHR and 179 tight junctions from cortices of nine WKY were investigated.

2.7. Tracer studies using lanthanum nitrate

For examination of para- and transcellular permeability, lanthanum nitrate was infused as a low molecular weight tracer (433 Da) [3]. The animals were anesthetized with intraperitoneal Ketanest/Rompun (Bayer AG, Germany) and intracardial perfusion was performed with Ringer solution containing heparin to avoid coagulation of blood cells. Subsequently, lanthanum nitrate solution in combination with fixative (HMSS pH 7.4, 1% lanthanum nitrate, 4% paraformaldehyde, 1% glutaraldehyde) was perfused and allowed to circulate for 20 min. Thereafter, the animals were sacrificed and the brains were removed, immersion fixed for 1 h (2.5% buffered glutaraldehyde) and subsequently processed for electron microscopy.

2.8. Statistical analysis

The statistical analysis was done using one-way ANOVA and Scheffè-test.

3. Results

3.1. Morphology of brain capillaries

We first used transmission electron microscopy to analyze endothelial cell junctions in cerebral capillaries. Ultrathin sections in SHRSP, SHR and WKY cortices revealed normal endothelial cells with only a low number of pinocytotic vesicles; the normal inter-endothelial junctions frequently contained tight junction occlusions. At these sites, the intercellular clefts showed closely opposed membranes of neighboring endothelial cells (Fig. 1a, b, c). Additionally, basal laminae, pericytes and astrocytic endfeet appeared to be normal. There was no morphological difference in the ultrastructure of blood–brain barrier endothelial cells between asymptomatic SHRSP, SHR and control WKY rats.

3.2. Freeze fracture analysis

The tight junctions of the blood–brain barrier endothelial cells of SHRSP, SHR and WKY rats shared the same level of complexity as indicated by a fractal dimension (box counting; $\log N/\log(1/s)$, where 'N' is the number of boxes containing TJ-structures and 's' is the scaling-factor; for details see Material and methods) of 1.67 ± 0.14, 1.58 ± 0.09 and 1.72 ± 0.12, respectively. In contrast, a dramatic difference was detected, considering the association of the tight junction particles to E- and P-face (Fig. 2a–f). Whereas in WKY rats, the P-face association of endothelial tight junction particles was consistently $58.7\pm3.6\%$ and in SHR rats $53.2\pm19.28\%$, in SHRSP rats two distinct populations of tight junctions could be observed. In a fraction of 27.8% of all investigated capillaries the P-face association was strongly decreased down to $10.5\pm5.1\%$ ($P<0.01$) (Fig. 2g). In the second population containing 72.2% of all observed intracerebral capillary tight junctions, the P-face association was as high as in WKY and SHR rats. The decrease in P-face associated particles in the first population was completely compensated by an increase in the number of particles on the E-face $89.4\pm9.9\%$ ($P<0.01$) (Fig. 2e–g). Thus, the total density of tight junction particles in SHRSP, SHR and WKY rats is approximately 100%, which was indicative for maintenance of tight junction integrity also in SHRSP rats.

3.3. Transmembrane and cytoplasmic proteins in endothelial cell–cell junctions

Antibodies against ZO-1, occludin, claudin-1 and claudin-5 were used for the identification of tight junction proteins. Immunoreactivities were present in cerebral microvessels labeling the margins of the endothelial cells at cell contacts. There was no difference in labeling intensity or localization between the SHRSP, SHR and the

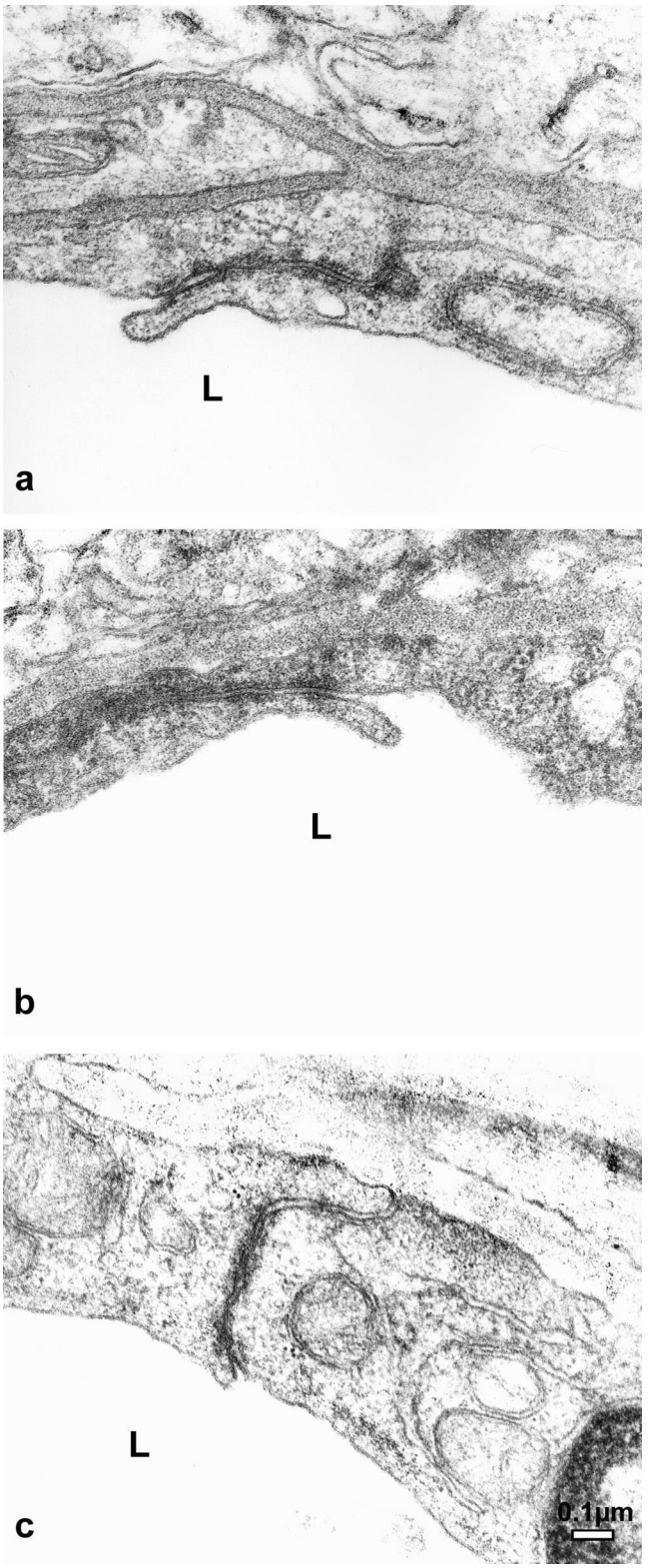

Fig. 1. Ultrathin section of a representative capillary in the cortex of WKY (a), SHR (b) and SHRSP (c). The endothelial cells have normal morphology with only a small number of pinocytotic vesicles and normal interendothelial junctions which frequently contain tight junction kisses. The intercellular clefts show closely opposed membranes of neighboring endothelial cells. (L, lumen); Magnification: (a–c) 1:60,000.

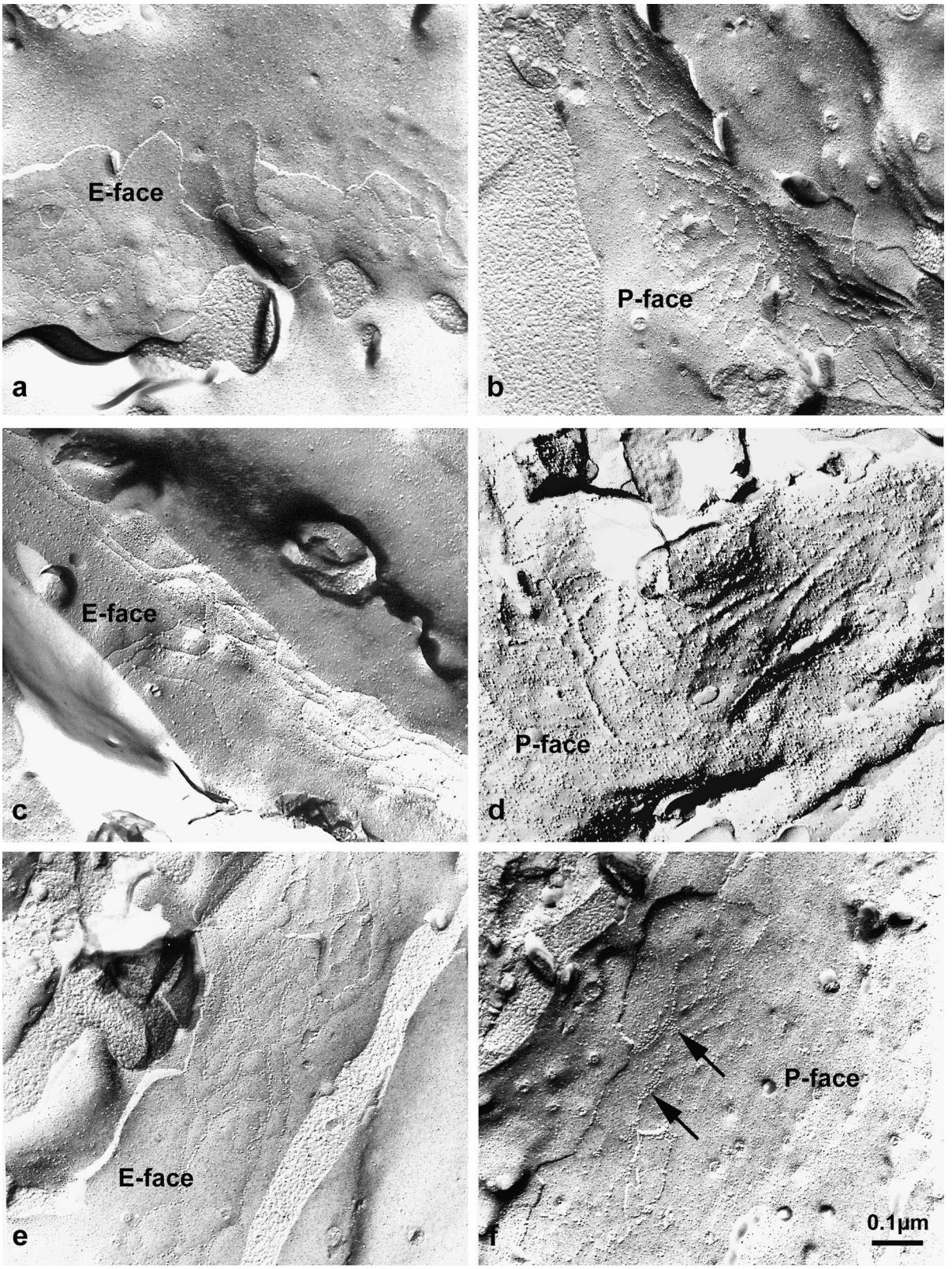

Fig. 2. Freeze-fracture electronmicrographs of tight junction strands in capillaries of cerebral cortices. The figure shows E-face (a, c, e) and P-face (b, d, f) leaflets of WKY (a, b), SHR (c, d) and SHRSP (e, f) capillaries. The arrows in (f) point to particle aggregates only observed in SHRSP capillaries, which may be an indicator for tight junction dynamic. (g) The E-face association of tight junction particles was markedly increased in SHRSP capillaries to about 89% ($P<0.01$) compared to WKY and SHR, whereas the P-face association was decreased to about 10% ($P<0.01$) (e and f). Magnification: 1:90,000.

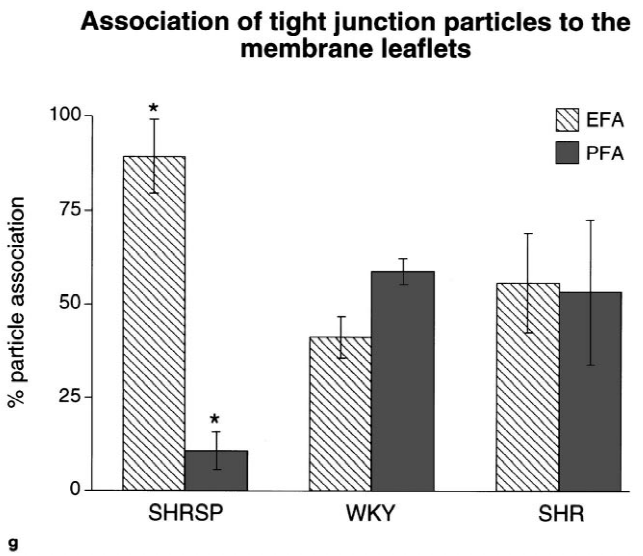

Fig. 2. (*continued*)

WKY brain microvessels (Fig. 3). ZO-1 (Fig. 3a–c) and occludin (Fig. 3d–f) shared the same distribution pattern and intensity in SHRSP, SHR and WKY strains. Both antigens were exclusively found in the junctional regions of blood–brain barrier endothelial cells. Claudin-5 immunoreactivity was found to share the same distribution pattern as occludin at the junctional membranes in all strains investigated (Fig. 3g–i). The claudin-1 immunoreactivity was weaker as that of the other tight junction molecules in the blood–brain barrier endothelial cells of all three rat strains (Fig. 3j–l).

3.4. Lanthanum nitrate permeability

Perfusion experiments using lanthanum nitrate as an electron-dense tracer did not result in any staining of the subendothelial space and there was no difference between SHRSP and WKY rats. The distribution of tracer deposits in the intercellular space stopped precisely where tight junctions were observed (Fig. 4a, b). Tracer deposits in adjacent tissue were seen exclusively in peripheral organs such as skeletal muscle (Fig. 4c), but not in the brain. Lanthanum nitrate deposits at the luminal surface of the capillaries were visible when the tracer was perfused together with the fixative.

3.5. Endothelial cell polarity

To investigate endothelial cell polarity, we studied the distribution of Glut-1 in the blood–brain barrier. We performed a quantitative evaluation of Glut-1 subcellular distribution across the luminal and abluminal surfaces of brain capillary endothelial cells. In WKY, we observed the typical asymmetric distribution of Glut-1 characteristic for the blood–brain barrier. The abluminal membrane was four-fold more heavily labeled than the luminal membrane (Fig. 5a, c). In contrast, blood–brain barrier capillaries of SHRSP rats consistently showed a sharp decrease in the abluminal/luminal gradient of Glut-1 density (Fig. 5b, c). While the cytoplasmic pool of anti-Glut-1 immunoreactivity was identical to that in control rats, the density of immunogold particles at the abluminal membrane decreased significantly ($P<0.05$) to $45\pm15.9\%$ in comparison to controls. The density of immunogold particles at the luminal membrane increased to $30.9\pm11.7\%$ ($P<0.05$) (Fig. 5c). Thus the polarity of cerebrovascular endothelial cells as defined as the abluminal/luminal distribution of the Glut-1, had decreased from 4 to about 1.4 under the hypertensive conditions in SHRSP.

4. Discussion

We tested the hypothesis that early changes in the composition of the junctional proteins may influence endothelial cell function in the blood–brain barrier in SHRSP. We showed by freeze-fracture technique that the morphology of the cell–cell contacts was altered. However, these changes in cell–cell contact in those young asymptomatic rats did not lead to detectable changes in permeability. Instead, they were associated with a loss of endothelial cell polarity. Still, the immunoreactivities of tight junction components such as ZO-1, occludin, claudin-1 and claudin-5 were unaltered.

We used electron microscopy to analyze endothelial tight junctions in SHRSP. The freeze-fracture technique is a powerful method to characterize tight junction structure and complexity. The method has been widely used for studies on blood–brain barrier development as well as for tight junction regulation in epithelia. The common agreement is that the tight junction particles of partner strands are separated by the membrane cleavage used in this method [14,20]. Tight junctions of blood–brain barrier endothelial cells show high protoplasmic face (P-face) association, whereas non-barrier blood vessels show a high external fracture face (E-face) association [28,44]. In an intact blood–brain barrier, about 57% of the observed particles are found in the P-face of the membrane whereas about 44% of the protein particles belong to the E-face [19]. It is now generally accepted that a switch of tight junctional particles in the brain capillary endothelial cells from the P- to the E-face correlates with an increase of the transendothelial permeability [39,44]. In contrast to normotensive animals and SHR, we observed an increased E-face association in SHRSP. This predominant E-face association resembled the one in blood–brain barrier during rat brain development [19] or in peripheral blood vessels [28]. Recently, many tight junction-associated proteins have been identified, including the claudin superfamily, occludin, and ZO-1 [6,23,25,26,34,40]. Occludin and claudins have functional relevance for intercellular

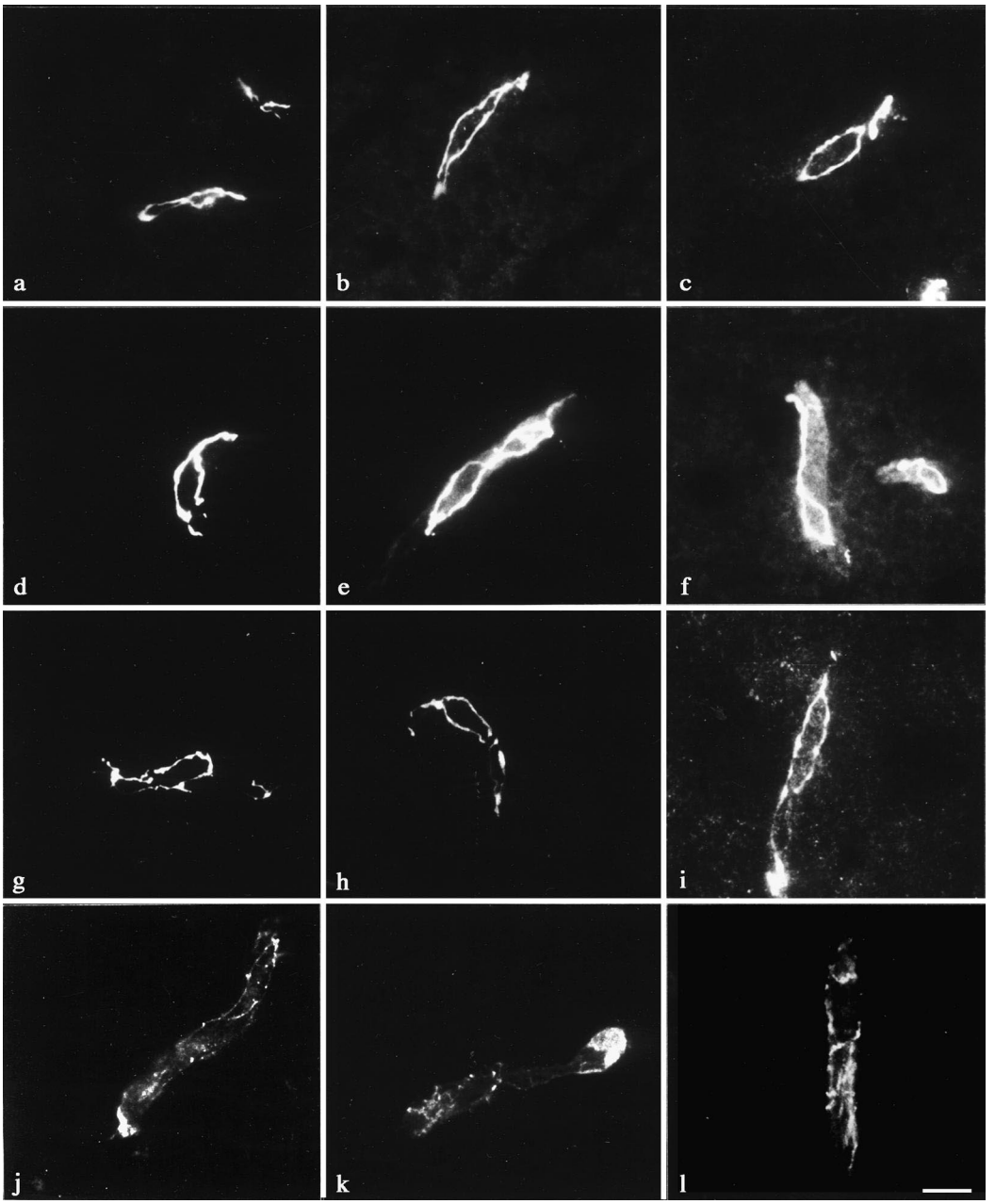

Fig. 3. Immunoreactivity of tight junction proteins in WKY (a, d, g, j), SHRSP (b, e, h, k) and SHR (c, f, i, l). Antibodies against ZO-1, occludin and claudin-1 and claudin-5 were used. ZO-1 (a–c) and occludin (d–f) share the same distribution pattern and intensity in WKY, SHRSP and SHR strains. Both antigens were exclusively found in the junctional regions of blood–brain barrier endothelial cells. Claudin-5 immunoreactivity was also observed at the margins of the endothelial cells with no difference between the rat strains (g–i). Claudin-1 immunoreactivity was weaker but also not different between the strains (j–l). Scale bar=6 μm.

adhesion and the paracellular barrier [11,25,34,40]. Claudin-1 and -5 were shown to induce the formation of tight junctions when transfected to fibroblasts normally lacking tight junctions [12,26]. Tight junctions formed after transfection with claudin-1 were associated largely with the P-face, whereas tight junctions formed after transfection with claudin-5 were associated with the E-face [12,26].

In the brain, the only claudins to be found are claudin-1, -5 and -11. Claudin-11/OSP was identified in oligodendrocytes [27], so that claudins-1 and -5, beside occludin, appear to be the most important structural components of blood–brain barrier tight junctions [21]. It has been hypothesized that the permeability-related quality of blood–brain barrier tight junctions might essentially depend on the ratio of claudin-1 to claudin-5 [21]. In the SHRSP rat, we found a dramatic increase of the tight junction particles associated with the E-face, thus indicat-

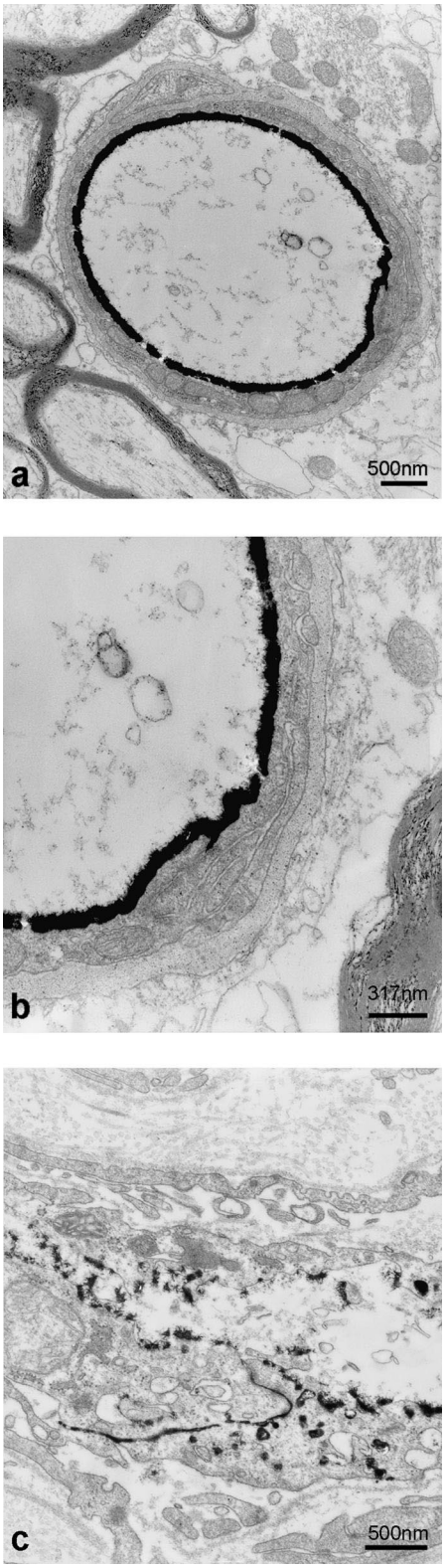

Fig. 4. Lanthanum nitrate was used to detect permeability changes in cerebral capillaries of SHRSP. The distribution of the tracer deposits stopped precisely where the tight junctions were observed in brain cerebral capillaries (a, b). (b) is a higher magnification of the tight junction area shown in (a) (box). In skeletal muscle used as a control tissue, the tracer crossed the intercellular space between the endothelial cells (c). Magnification: (a) 1:13,000; (b) 1:25,000; (c) 1:18,000.

ing that the intracellular tight junction regulation may be altered in genetic hypertension. Despite the structural changes, we did neither observe a changed claudin-1 and claudin-5 expression, respectively, nor an increase in endothelial permeability. This is in contrast to observations made in transfection experiments where E-face associated tight junctions are composed mainly of claudin-5 particles and P-face-associated tight junctions of claudin-1 particles [12,26]. We hypothesize that under the investigated pathological conditions not changes in gene expression but rather signalling events are responsible for the particle shift to the other fracture face. Permeability studies using horseradish peroxidase or Evans blue, a marker for albumin permeability, have been done in older SHRSP after the onset of stroke [9,10,13,37]. In contrast, we studied asymptomatic SHRSP at 13 weeks of age, which is before the onset of major changes in cerebral vessel morphology and before the blood pressure maximum is reached. However, at this stage, there was no increased permeability to lanthanum nitrate and it seems reasonable to assume that early changes in endothelial permeability cannot be detected by lanthanum nitrate perfusion and we suggest that electron microscopically detectable changes in endothelial permeability are a later phenomenon in the development of stroke. This assumption is supported by the observation that in experimental diabetic retinopathy, no increase in lanthanum permeability in retinal pigment epithelial cells has been observed in early disease. This was despite of tight junctions that are characterized by an increased E-face association [3]. Obviously, ultrastructural changes in tight junctions precede alterations in permeability. As the tight junctional alterations described in this study cannot be explained by an increased capillary pressure, since it has been found to be near normal in SHRSP rats [8], we cannot rule out signals from the blood to the capillary wall originating from a changed metabolism under hypertensive conditions. Thus a direct influence of blood pressure on the blood–brain barrier properties is highly unlikely. Alternatively the observed changes in the endothelial cells of the blood–brain barrier could also be induced by the adjacent astrocytes. Astrocytes are generally believed to be important for the induction of the blood–brain barrier [16,32,33,44]. As well, astrocytes from SHRSP were described to be involved in the induction of an impaired endothelial barrier in vitro [45]. The same phenomenon was also observed in astrocytes from glial fibrillary acidic protein (GFAP) knock out mice that were not able to induce blood–brain barrier properties in vitro [31] as well as in vivo [22].

Finally, we observed an altered endothelial cell polarity, as assessed by Glut-1 distribution. Glut-1 and its subcellular distribution is a specific marker for blood–brain barrier endothelial cells. Glut-1 is asymmetrically distributed in the cerebral microvasculature; the appearance of this asymmetry is a specific parameter for the developing blood–brain barrier [1,7]. The asymmetric distribution

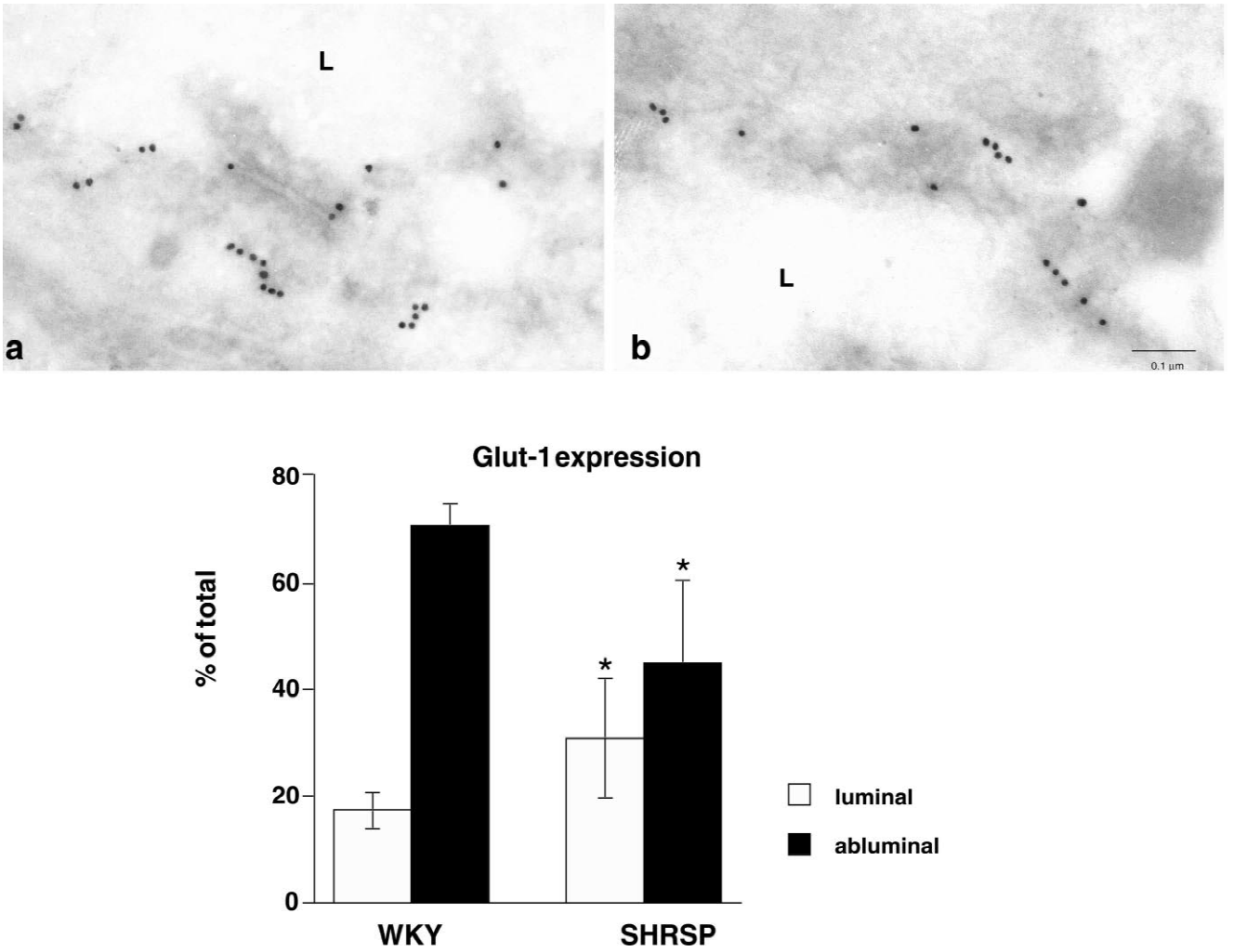

Fig. 5. Glut-1 immunoreactivity in cerebral capillaries of WKY (a) and SHRSP (b) demonstrated by immunogold labeling. In WKY rats we observed the typical asymmetric distribution of Glut-1. The abluminal membrane was four-fold heavier labeled than the luminal membrane (a, c). In contrast, blood–brain barrier capillaries of SHRSP rats consistently showed a sharp decrease of the abluminal/luminal gradient of Glut-1-density (b, c). Whereas the cytoplasmic pool of anti-Glut-1 immunoreactivity was identical to that in the control rat, the density of immunogold particles at the abluminal membrane decreased significantly to 45% in comparison to the control ($P<0.05$), and the density of immunogold particles at the luminal membrane increased to 30.8% ($P<0.05$) (c). Magnification (a) and (b): 1:90,000.

seems to be regulated by the fence function of the tight junctions. It is not contradictory that we find a reduced endothelial Glut-1-related polarity in all capillary profiles investigated, and an increase of the E-face association of tight junction particles in only 27.8% of the tight junctions analysed. A given replica cannot show the whole tight junction of the appropriate cell. Therefore, 27.8% of altered tight junctions do not reflect 27.8% of endothelial cells with an altered fence function. One gap in the tight junction network which may only improbably be detected by freeze-fracturing may lead to a considerable change in gate and fence functions of the cells.

Our data suggest that the tight junction structural changes may lead to reduced abluminal Glut-1-transporter molecule density and an increase in the luminal density. The data further suggest disturbed cytoskeletal link and fence function in the junctional proteins. Moreover, the altered fracture face distribution of tight junction molecules may influence the blood–brain barrier maintenance in genetic hypertension. We do not yet know if the observed changes are induced by the developing hypertension in these rats or if they are genetically determined. The issue requires further investigation.

In conclusion, we have demonstrated that in SHRSP rats the blood–brain barrier capillary endothelial cell tight junctions show, prior to the manifestation of stroke, the same alterations, namely an increase of the E-face association, which previously were discussed to indicate an increased permeability and/or decreased barrier function under different conditions of injuries. The decrease of the Glut-1-related endothelial polarity may be a consequence of this barrier alteration. Further studies have to clarify which molecular mechanisms are responsible for the effect of hypertension on the immediate decrease of the fence

function and the delayed decrease of the gate function in blood–brain barrier endothelial cells in vivo.

The observed alterations point toward changes in endothelial cells induced by yet unknown influences that predispose these rats to stroke induced blood–brain barrier break down rather than being the reason for stroke in SHRSP.

Acknowledgements

This study was supported by a grant-in-aid from the Deutsche Forschungsgemeinschaft to Andrea Lippoldt and Hermann Haller (DFG, Li 604/2-1) and from the Deutsche Krebshilfe to Stefan Liebner and Hartwig Wolburg (10-1282-Wo I). We are grateful to Heike Thränhardt and Heike Michael for technical assistance and to Detlev Ganten and Friedrich C. Luft for critically reading the manuscript.

References

[1] S. Bolz, C.L. Farrell, K. Dietz, H. Wolburg, Subcellular distribution of glucose transporter (GLUT-1) during development of the blood–brain barrier in rats, Cell Tiss. Res. 284 (1996) 355–365.
[2] M.W. Brightman, I. Klatzo, Y. Olsson, T.S. Reese, The blood–brain barrier to proteins under normal and pathological conditions, J. Neurol. Sci. 10 (1970) 215–239.
[3] R.B. Caldwell, S.M. Slapnick, B.J. McLaughlin, Lanthanum and freeze-fracture studies of retinal pigment epithelial cell junctions in the streptozotocin diabetic rat, Curr. Eye Res. 14 (1985) 215–227.
[4] G.A. Donnan, A. Thrift, R.X. You, J.J. McNeill, Hypertension and stroke, J. Hypertens. 12 (1994) 865–869.
[5] A.E. Doyle, G.A. Donnan, Stroke as a critical problem in hypertension, J. Cardiovasc. Pharmacol. 15 (Suppl. 1) (1990) S34–S37.
[6] A.S. Fanning, B.J. Jameson, L.A. Jesaitis, J.M. Anderson, The tight junction protein ZO-1 establishes a link between the transmembrane protein occludin and the actin cytoskeleton, J. Biol. Chem. 273 (1998) 29745–29753.
[7] C.L. Farrell, W.M. Pardridge, Blood–brain barrier glucose transporter is asymmetrically distributed on brain capillary endothelial lumenal and ablumenal plasma membranes: an electron microscopic immunogold study, Proc. Natl. Acad. Sci. USA 88 (1991) 779–783.
[8] K. Fredriksson, M. Ingvar, B.B. Johansson, Regional cerebral blood flow in conscious stroke-prone spontaneously hypertensive rats, J. Cerebr. Blood Flow Metab. 4 (1984) 103–106.
[9] K. Fredriksson, R.N. Auer, H. Kalimo, C. Nordborg, Y. Olsson, B.B. Johansson, Cerebrovascular lesions in stroke-prone spontaneously hypertensive rats, Acta Neuropathol. (Berl.) 68 (1985) 284–294.
[10] K. Fredriksson, H. Kalimo, C. Nordborg, Y. Olsson, B.B. Johansson, Cyst formation and glial response in the brain lesions of stroke-prone spontaneously hypertensive rats, Acta Neuropathol. (Berl.) 76 (1988) 441–450.
[11] M. Furuse, T. Hirase, M. Itoh, A. Nagafuchi, S. Yonemura, S. Tsukita, S. Tsukita, Occludin: a novel integral membrane protein localizing at tight junctions, J. Cell Biol. 123 (1993) 1777–1788.
[12] M. Furuse, H. Sasaki, K. Fujimoto, S. Tsukita, A single gene product, claudin-1 or -2, reconstitutes tight junction strands and recruits occludin in fibroblasts, J. Cell Biol. 143 (1998) 391–401.
[13] F. Hazama, S. Amano, H. Haebara, K. Okamoto, Changes in vascular permeability in the brain of stroke-prone spontaneously hypertensive rats studied with peroxidase as a tracer, Acta Pathol. Jap. 25 (1975) 565–574.
[14] N. Hirokawa, The intramembrane structure of tight junctions. An experimental analysis of the single-fibril and two-fibrils models using the quick-freeze method, J. Ultrastr. Res. 80 (1982) 288–301.
[15] K. Ikeda, Y. Nara, C. Matumoto, T. Mashimo, T. Tamada, M. Sawamura, T. Nabika, Y. Yamori, The region responsible for stroke on chromosome 4 in the stroke-prone spontaneously hypertensive rat, Biochem. Biophys. Res. Commun. 229 (1996) 658–662.
[16] R.C. Janzer, M.C. Raff, Astrocytes induce blood–brain barrier properties in endothelial cells, Nature 325 (1987) 253–257.
[17] B.B. Johansson, The blood–brain barrier in acute and chronic hypertension, Adv. Exp. Med. Biol. 131 (1980) 211–226.
[18] U. Kniesel, A. Reichenbach, W. Risau, H. Wolburg, Quantification of tight junction complexity by means of fractal analysis, Tissue Cell 26 (1994) 901–912.
[19] U. Kniesel, W. Risau, H. Wolburg, Development of blood–brain barrier tight junctions in the rat cortex, Dev. Brain Res. 96 (1996) 229–240.
[20] N.J. Lane, T.J. Reese, B. Kachar, Structural domains of the tight junctional intramembrane fibrils, Tissue Cell 24 (1992) 291–300.
[21] S. Liebner, A. Fischmann, G. Rascher, F. Duffner, E.H. Grote, H. Kalbacher, H. Wolburg, Claudin-1 and claudin-5 expression and tight junction morphology are altered in blood vessels of human glioblastoma multiforme, Acta Neuropathol. 100 (2000) 323–331.
[22] W. Liedtke, W. Edelman, P.L. Bieri, F.C. Chiu, N.J. Cowan, R. Kucherlapati, C.S. Raine, GFAP is necessary for the integrity of CNS white matter architecture and long-term maintenance of myelination, Neuron 17 (1996) 607–615.
[23] K.M. McCarthy, I.B. Skare, M.C. Stankewich, M. Furuse, S. Tsukita, R.A. Rogers, R.D. Lynch, E.E. Schneeberger, Occludin is a functional component of the tight junction, J. Cell Sci. 109 (1996) 2287–2298.
[24] G. Mies, D. Hermann, U. Ganten, K.A. Hossmann, Hemodynamics and metabolism in stroke-prone spontaneously hypertensive rats before manifestation of brain infarcts, J. Cerebr. Blood Flow Metab. 19 (1999) 1238–1246.
[25] K. Morita, M. Furuse, K. Fujimoto, S. Tsukita, Claudin multigene family encoding four-transmembrane domain protein components of tight junction strands, Proc. Natl. Acad. Sci. USA 96 (1999) 511–516.
[26] K. Morita, H. Sasaki, M. Furuse, S. Tsukita, Endothelial claudin: claudin-5/TMVCF constitutes tight junction strands in endothelial cells, J. Cell Biol. 147 (1999) 185–194.
[27] K. Morita, H. Sasaki, K. Fujimoto, M. Furuse, S. Tsukita, Claudin 11/OSP-based tight junctions in myelinated sheaths of oligodendrocytes and Sertoli cells in testis, J. Cell Biol. 145 (1999) 579–588.
[28] H. Mühleisen, H. Wolburg, E. Betz, Freeze-fracture analysis of endothelial cell membranes in rabbit carotid arteries subjected to short-term atherogenic stimuli, Virch. Arch. B Cell Pathol. 56 (1989) 413–417.
[29] Y. Nishimura, A. Suzuki, Relaxant effects of vasodilator peptides on isolated basilar arteries from stroke-prone spontaneously hypertensive rats, Clin. Exp. Pharmacol. Physiol. 24 (1997) 157–161.
[30] W. Paschen, G. Mies, W. Bodsch, Y. Yamori, K.A. Hossmann, Regional cerebral blood flow, glucose metabolism, protein synthesis, serum protein extravasation, and content of biochemical substrates in stroke-prone spontaneously hypertensive rats, Stroke 16 (1985) 841–845.
[31] M. Pekny, K. Stannes, C. Eliasson, C. Betsholtz, D. Janigro, Impaired induction of blood–brain barrier properties in aortic endothelial cells by astrocytes from GFAP-deficient mice, Glia 22 (1998) 390–400.
[32] W. Risau, H. Wolburg, Development of the blood-brain barrier, Trends Neurosci. 13 (1990) 174–178.
[33] L.L. Rubin, D.E. Hall, S. Porter, K. Barbu, C. Cannon, H.C. Horner, M. Janatpour, C.W. Liaw, K. Manning, J. Morales, L.I. Tanner, K.J.

Tomaselli, F. Bard, A cell culture model of the blood–brain barrier, J. Cell Biol. 115 (1991) 1725–1735.
[34] M. Saitou, K. Fujimoto, Y. Doi, M. Itoh, T. Fujimoto, M. Furuse, H. Takano, T. Noda, S. Tsukita, Occludin-deficient embryonic stem cells can differentiate into polarized epithelial cells bearing tight junctions, J. Cell Biol. 141 (1998) 397–408.
[35] C.T. Stier Jr., N. Selig, H.D. Itskovitz, Enhanced vasodilatory responses to bradykinin in stroke-prone spontaneously hypertensive rats, Eur. J. Pharmacol. 210 (1992) 217–219.
[36] S. Strandgaard, O.B. Paulson, Pathophysiology of stroke, J. Cardiovasc. Pharmacol. 15 (Suppl. 1) (1990) S38–S42.
[37] M. Tagami, Y. Nara, A. Kubota, H. Fujino, Y. Yamori, Ultrastructural changes in cerebral pericytes and astrocytes of stroke-prone spontaneously hypertensive rats, Stroke 21 (1990) 1064–1071.
[38] M. Tagami, A. Kubota, T. Sunaga, H. Fujino, H. Maezawa, M. Kihara, Y. Nara, Y. Yamori, Increased transendothelial channel transport of cerebral capillary endothelium in stroke-prone SHR, Stroke 14 (1983) 591–596.
[39] S. Tsukita, M. Furuse, Occludin and claudins in tight junction strands: leading or supporting players?, Trends Cell Biol. 9 (1999) 268–273.
[40] C.M. Van Itallie, J.M. Anderson, Occludin confers adhesiveness when expressed in fibroblasts, J. Cell Sci. 110 (1997) 1113–1121.
[41] M. Volpe, G. Iaccarino, C. Vecchione, D. Rizzoni, R. Russo, S. Rubattu, G. Condorelli, U. Ganten, D. Ganten, B. Trimarco, K. Lindpaintner, Association and cosegregation of stroke with impaired hypertensive rats, J. Clin. Invest. 98 (1996) 256–261.
[42] A.W. Vorbrodt, Morphological evidence of the functional polarization of brain microvascular endothelium, in: W.M. Pardrige (Ed.), The Blood–Brain Barrier, Raven Press Ltd, New York, 1993, pp. 137–164.
[43] A.W. Vorbrodt, A.S. Lossinsky, H.M. Wisniewski, R. Suzuki, T. Yamaguchi, H. Masaoka, I. Klatzo, Ultrastructural observations on the transvascular route of protein removal in vasogenic brain edema, Acta Neuropathol. (Berl.) 66 (1985) 265–273.
[44] H. Wolburg, J. Neuhaus, U. Kniesel, B. Krauss, E.-M. Schmid, M. Öcalan, C. Farrell, W. Risau, Modulation of tight junction structure in blood–brain barrier endothelial cells. Effect of tissue culture, second messengers and cocultured astrocytes, J. Cell Sci. 107 (1994) 1347–1357.
[45] K. Yamagata, M. Tagami, Y. Nara, H. Fujino, A. Kubota, F. Numano, T. Kato, Y. Yamori, Faulty induction of blood–brain barrier functions by astrocytes isolated from stroke-prone spontaneously hypertensive rats, Clin. Exp. Pharmacol. Physiol. 24 (1997) 686–691.
[46] Y. Yamasaki, Y. Yamamoto, Y. Senga, M. Isogai, H. Shimizu, Y. Yamori, Decreased cerebral metabolism in stroke-prone spontaneously hypertensive rats (SHRSP) with stroke and its possible improvement by Solcoseryl, Clin. Exp. Hypertens. [A] 13 (1991) 1051–1057.
[47] Y. Yamori, R. Horie, I. Akiguchi, M. Kihara, Y. Nara, W. Lovenberg, Symptomatical classification in the development of stroke in stroke-prone spontaneously hypertensive rats, Jap. Circ. J. 46 (1981) 274–283.
[48] Y. Yamori, Implication of hypertensive rat models for primordial nutritional prevention of cardiovascular diseases, Clin. Exp. Pharmacol. Physiol. 26 (1999) 568–572.
[49] S.T. Yang, W.G. Mayhan, F.M. Faraci, D.D. Heistad, Endothelium-dependent responses of cerebral blood vessels during chronic hypertension, Hypertension 17 (1991) 612–618.